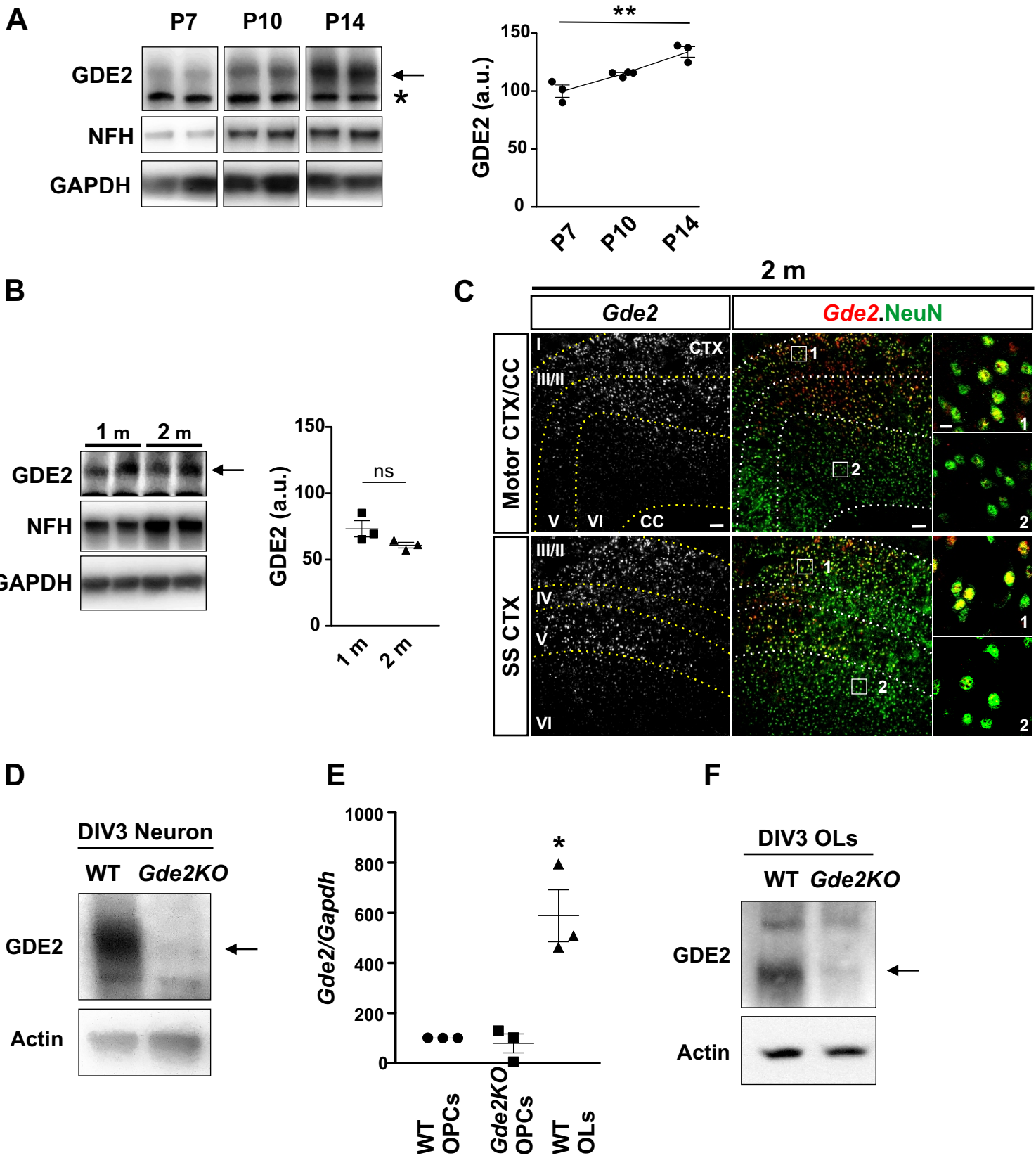


**Supplemental Information**

**GDE2-Dependent Activation  
of Canonical Wnt Signaling in Neurons  
Regulates Oligodendrocyte Maturation**

**Bo-Ran Choi, Clinton Cave, Chan Hyun Na, and Shanthini Sockanathan**

**Figure S1**



**Figure S1. Related to Figure 1. GDE2 is expressed in neurons and OLs.**

(A) Western blot of cortical extracts from WT animals at postnatal day 7 (P7), P10 and P14. GAPDH is a loading control, NFH is expressed in axons and provides a readout of neurons in brain tissue. Arrow indicates GDE2. Asterisk indicates a nonspecific band. Graph quantifying Western data from P7-P14. a.u. = arbitrary units. \*\*p = 0.0013. n = 3 P7, 4 P10, 3 P14, 1-way ANOVA. (B) Western blot and quantification of GDE2 protein expression at 1 and 2 months (m) of age. ns p = 0.182. n = 3 for each timepoint, two-tailed unpaired t-test. (C) Cortical coronal sections showing *Gde2* transcript distribution. CC: corpus callosum, SS: somatosensory cortex. Cortical layers are marked by dotted lines. Boxed areas 1 and 2 are magnified in right panels. Scale bar: 100 µm, insets 10 µm (D) Western blot of DIV3 cortical neuronal cultures. Arrow marks GDE2. Actin is a loading control. (E) qPCR of *Gde2* transcripts normalized to *Gapdh* mRNA. \*p = 0.0021. n = 3 sets of WT, *Gde2KO* OPCs, and WT OLs, 1-way ANOVA. (F) Western blot shows GDE2 is expressed in WT OLs (marked by arrow). Actin is a loading control. All graphs: Mean ± sem.

**Figure S2**

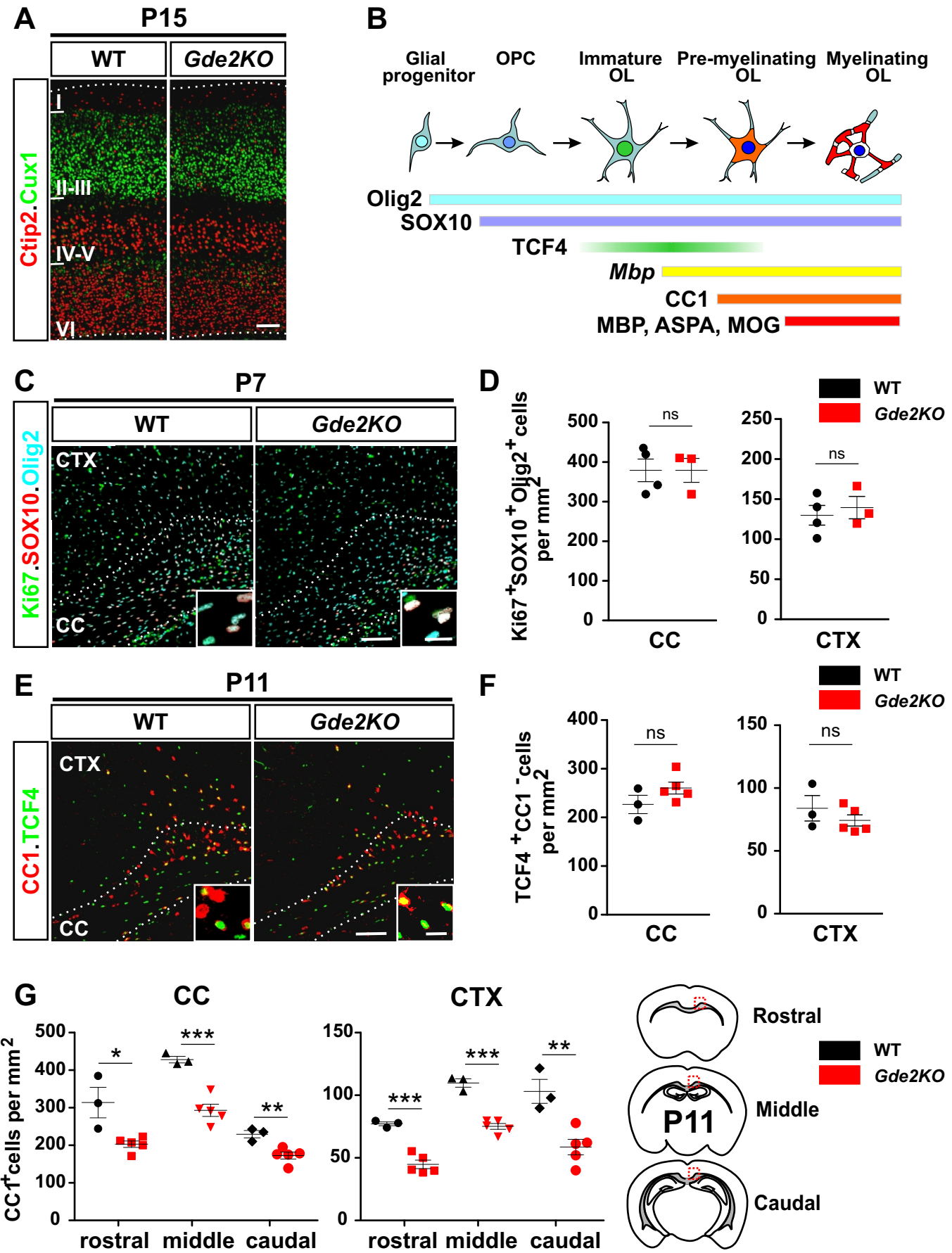


**Figure S2. Related to Figure 2. GDE2 loss impairs OL maturation.**

(A) Coronal section of P15 mouse cortex, hatched lines mark cortical boundaries. Cortical layers I-VI are marked. (B) Schematic showing the progression of OL maturation coincident with marker expression. (C) Coronal section of P7 mouse cortex (CTX) and corpus callosum (CC). Hatched line marks boundary between CTX and CC. Inset box shows magnified image of proliferating OPCs (white, Ki67+Sox10+Olig2+). (D) Graphs quantifying the number of proliferating OPCs (Ki67+Sox10+Olig2+) CC ns p = 0.9981 and CTX ns p = 0.6352, n = 4 WT, 3 *Gde2KO*. Two tailed unpaired Student's t-test. (E) Coronal section of P11 mouse CTX and CC. Hatched line demarcates the CC. Inset box shows magnified image of immature (TCF4+CC1-) and mature OLs (CC1+). (F) Graphs quantifying the number of immature OLs (TCF4+CC1-). CC ns p = 0.2306 and CTX ns p = 0.8021, n = 3 WT, 5 *Gde2KO*. Two tailed unpaired Student's t-test. (G) Graphs quantifying number of CC1+ cells in boxed areas in rostral, middle and caudal regions of mouse P11 CC and CTX as shown in schematic. Data for middle regions are the same as in Figure 2B and are reproduced here for comparison purposes. CC: \*p rostral = 0.013 \*\*\*p middle = 0.0007 \*\*p caudal = 0.0072; CTX: \*p rostral = 0.0004 \*\*\*p middle = 0.0035 \*\*p caudal = 0.0063. n = 3 WT 5 *Gde2KO*. Two tailed unpaired Student's t-test. All graphs: Mean  $\pm$  sem. Scale bars: (A, C, E) 100  $\mu$ m, insets (C, E) 5  $\mu$ m.

**Figure S3**

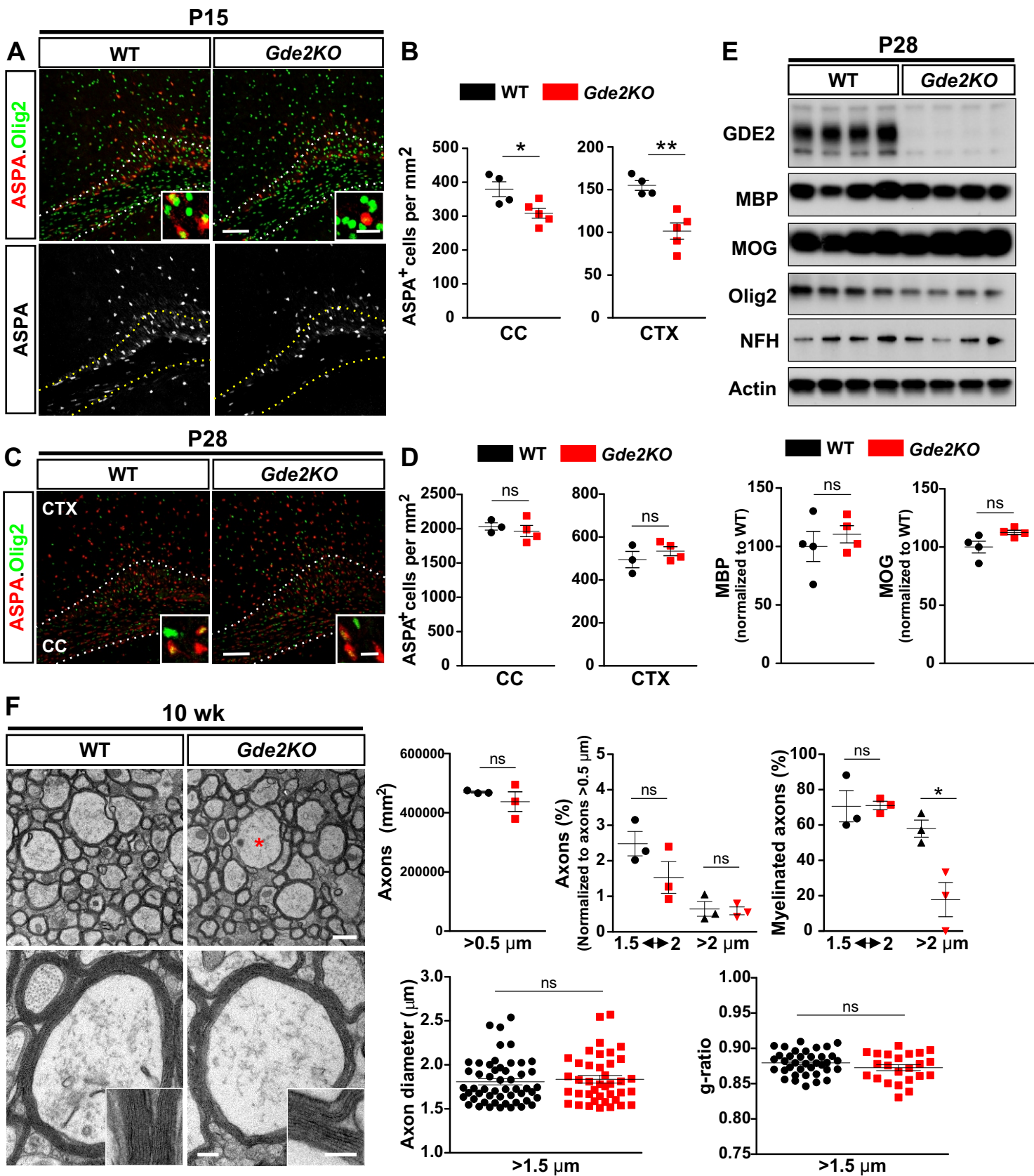


**Figure S3. Related to Figure 2. *Gde2* KOs show recovery of myelin protein but have decreased myelination of large-diameter axons.**

(A, C) Coronal sections of mouse cortex (CTX) and corpus callosum (CC). Hatched lines delineate the CC. Insets show high magnification of mature OLs. Scale bars: 100  $\mu\text{m}$  insets: 10  $\mu\text{m}$  in A and C. (B, D) Graphs quantifying numbers of ASPA+ OLs in CC and CTX. (B) CC \* $p$  = 0.0275 and CTX \*\* $p$  = 0.0028, n = 4 WT, 5 *Gde2KO* (D) CC ns  $p$  = 0.539 and CTX ns  $p$  = 0.4373, n = 3 WT, 4 *Gde2KO*. (E) Western blot of cortical extracts from P28 animals. Graphs quantifying myelin associated proteins MBP ns  $p$  = 0.5198, MOG ns  $p$  = 0.1035 n = 4 WT, 4 *Gde2KO*. (F) Representative TEM images of 10 week WT and *Gde2KO* animals. \* marks exemplar unmyelinated larger-diameter axon in *Gde2KO* condition. Scale bar: (Top) 1  $\mu\text{m}$ , (Bottom) 200 nm, Inset 100 nm. Graphs quantifying axon numbers (ns  $p$  = 0.3905) and the percentage of axons with diameters between 1.5 and 2  $\mu\text{m}$  (ns  $p$  = 0.1649) and larger than 2  $\mu\text{m}$  (ns  $p$  = 0.8323). Although the percentage of myelinated axons between 1.5 and 2  $\mu\text{m}$  is equivalent between WT and *Gde2KO* animals (ns  $p$  = 0.9667), the percentage of myelinated axons with diameters larger than 2  $\mu\text{m}$  is dramatically reduced (\* $p$  = 0.0206) n = 3 WT, 3 *Gde2KO*. Diameters of axons greater than 0.5  $\mu\text{m}$  (ns  $p$  = 0.5977) and g-ratios of myelinated axons with diameters larger than 1.5  $\mu\text{m}$  are unchanged between WT and *Gde2KO* animals (ns  $p$  = 0.156). Each point refers to individual myelinated axons from 3 WT and 3 *Gde2KO*. All graphs Mean  $\pm$  sem, two tailed unpaired t-test.

**Figure S4**

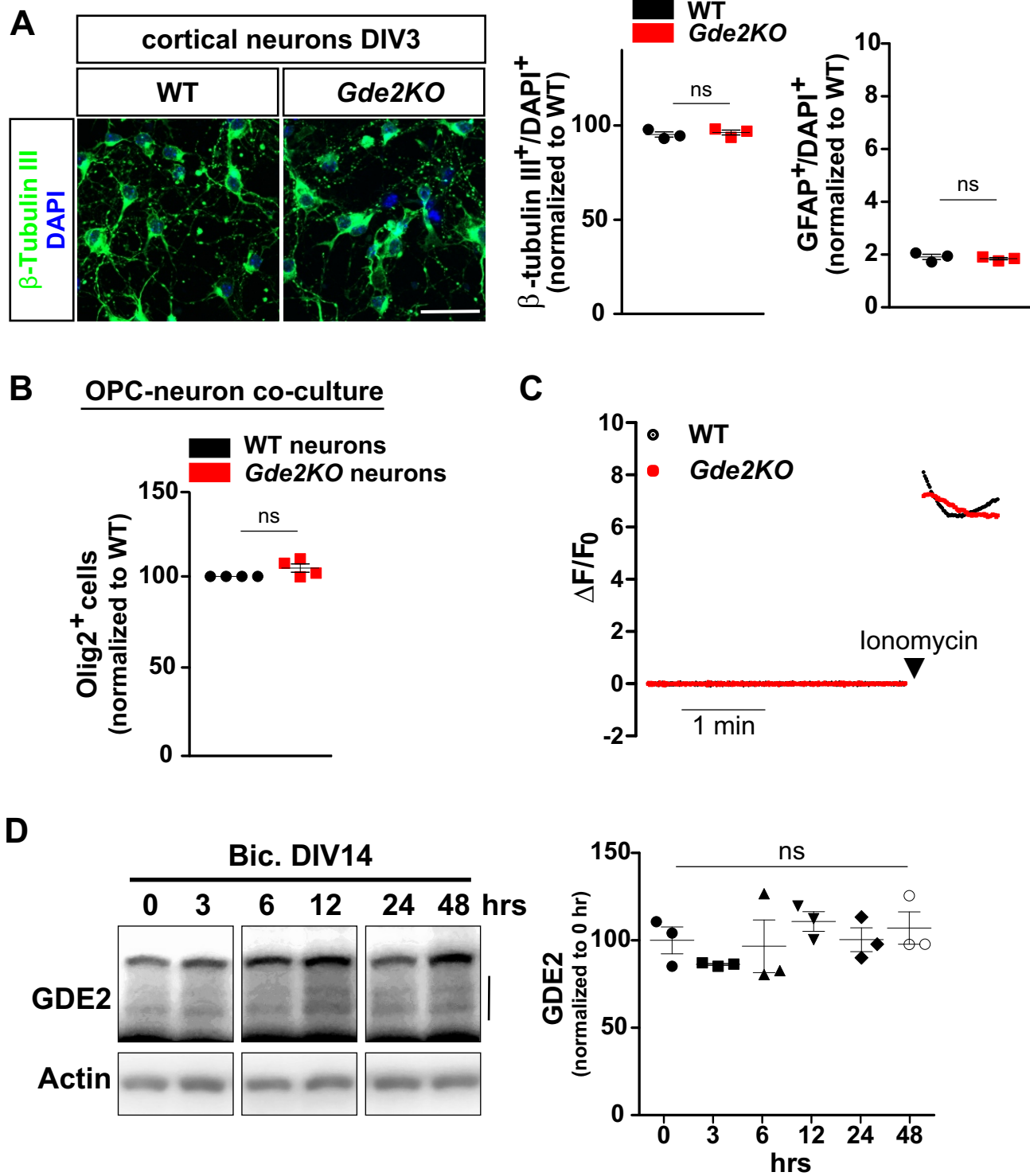


**Figure S4. Related to Figure 4. Characterization of neuron-OPC co-cultures.**

(A) Immunocytochemical staining of DIV3 cortical neuronal cultures. Scale bar: 50  $\mu$ m. Graphs quantifying percentage neurons ( $\beta$ -tubulin III+) and astrocytes in DIV3 WT and *Gde2KO* cortical neuronal cultures ( $\beta$ -tubulin III+ ns p = 0.6243; GFAP+ ns p = 0.6093; n = 3 WT 3 *Gde2KO*). (B) Graph quantifying the number of Olig2+ cells after neuron-OPC co-culture (ns p = 0.1235, n = 4 WT neuron-WT OPC co-cultures, 4 *Gde2KO* neuron-WT OPC co-cultures). Two tailed unpaired Student's t-test. All graphs: Mean  $\pm$  sem. (C) Graph of fluorescence changes ( $\Delta F/F_0$ ) in DIV3 WT and *Gde2KO* neurons loaded with the calcium indicator Fluo-4 over a 3.5 minute period. Each data point represents mean value of  $\Delta F/F_0$  from at least 11 recordings per group at a given time. Arrowhead marks the time of ionomycin addition, which permeabilizes the membrane and acts as a positive control. (D) Western blot of DIV14 cortical neurons treated with bicuculline for specified times. Bar denotes GDE2. Graph quantifying GDE2 protein levels show no change in expression after stimulation. 1 way ANOVA ns p = 0.4692, n = 3 for each timepoint.

**Figure S5**

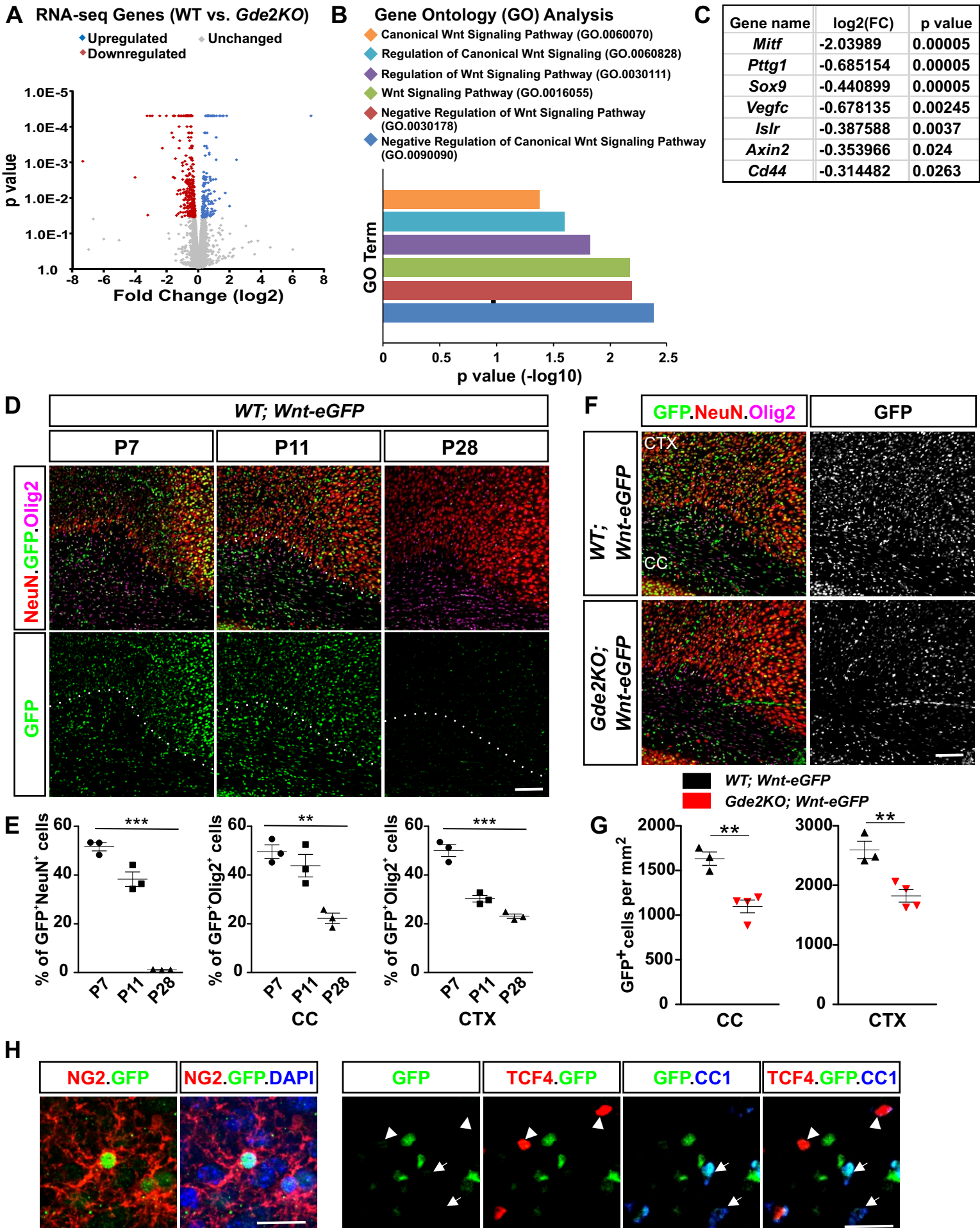


**Figure S5. Related to Figure 5. Canonical Wnt signaling is reduced when GDE2 is disrupted.**

(A) Volcano plot showing differentially expressed genes between WT and *Gde2KO* spinal cord. (B) Gene ontology analysis using p-value (< 0.05) highlights Wnt signaling pathways are disrupted in absence of GDE2. (C) List of known Wnt target genes that are altered in *Gde2KO* condition. (D) Analysis of Wnt-reporter animals (*Wnt-eGFP*) show that canonical Wnt signaling (eGFP) is high at P7 and P11 but is minimal at P28. Hatched line marks the boundary between cortex and corpus callosum. (E) Graphs quantifying the percentage of reporter gene expression in *Wnt-eGFP* mice at P7, P11 and P28 in neurons (NeuN+) and oligodendroglia (Olig2+) in corpus callosum (CC) and cortex (CTX). GFP+NeuN+ \*\*\*p < 0.0001, GFP+Olig2+ CC \*\*p = 0.0027, GFP+Olig2+ CTX \*\*\*p <0.0001. n = 3 P7, 3 P11, 3 P28, 1-way ANOVA. Data for P11 are the same as presented in Figure 4F and 4H (WT) and are included here for comparison purposes. (F) Coronal sections of P11 WT; *Wnt-eGFP* and *Gde2KO;Wnt-eGFP* animals (G) Graphs quantifying GFP+ cells in CC and CTX. CC \*\*p = 0.004, CTX \*\*p = 0.007, n = 3 WT; *Wnt-eGFP*, 4 *Gde2KO;Wnt-eGFP*, two-tailed unpaired t-test. (H) Representative image of P11 cortex of *Wnt-eGFP* mice. Arrowheads mark TCF4+CC1- immature OLs, arrows mark mature CC1+ OLs; both populations do not co-express eGFP. All graphs: Mean  $\pm$  sem. Scale bar: (D, F) 100  $\mu$ m, (H) 20 $\mu$ m.

## Figure S6

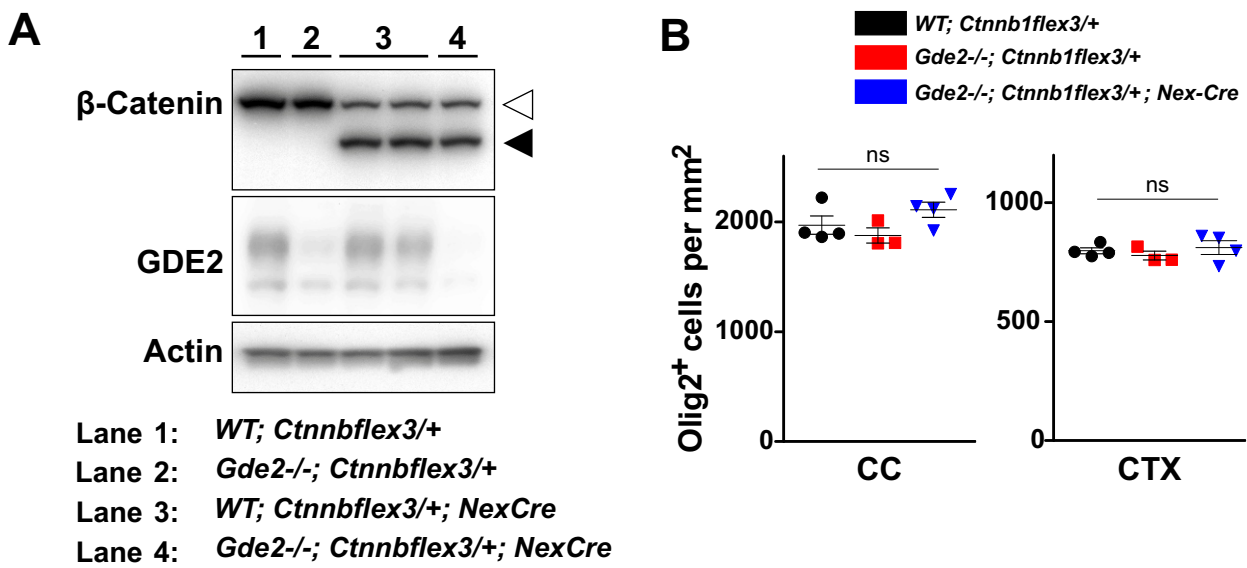


**Figure S6. Related to Figure 6. Genetic stabilization of  $\beta$ -catenin in neurons does not change total Olig2+ cells.**

(A) Western blot of P14 cortical extracts. Open arrowhead marks WT  $\beta$ -catenin; black arrowhead marks  $\beta$ -catenin deleted for exon 3. Actin is used as a loading control. (B) Graphs quantifying the number of Olig2+ cells in P11 corpus callosum (CC) and cortex (CTX). ns CC p = 0.1608 (1-way ANOVA/Bonferroni's multiple comparison test), ns CTX p = 0.6109 (1-way ANOVA/Bonferroni's multiple comparison test). n = 4 *WT;β-cat<sup>ex3</sup>*, 3 *Gde2KO;β-cat<sup>ex3</sup>*, 4 *Gde2KO;N-β-cat<sup>ex3</sup>*. All graphs: Mean  $\pm$  sem.

**Figure S7**

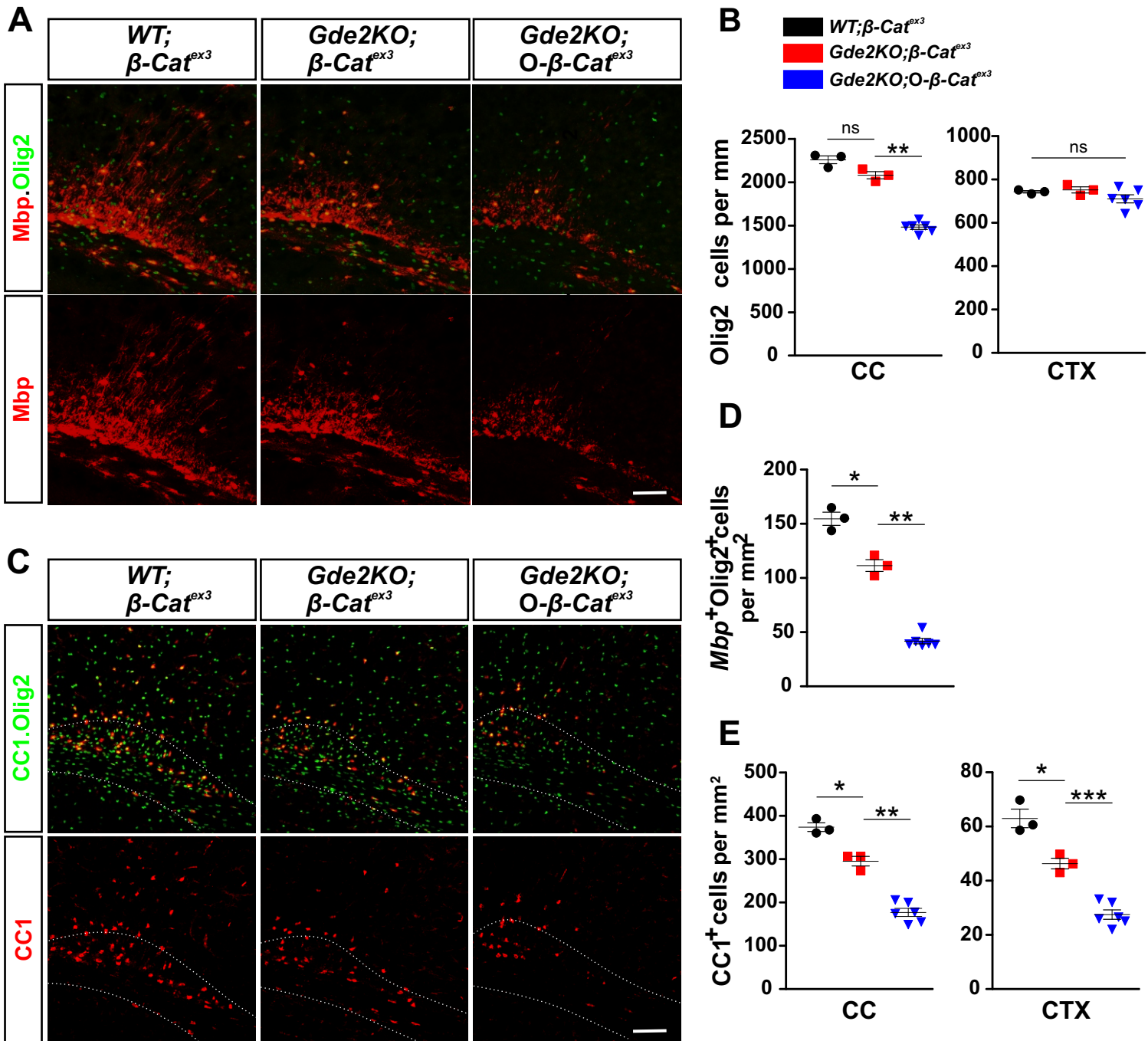


**Figure S7. Related to Figure 5. Stabilization of  $\beta$ -catenin in OPCs does not rescue *Gde2KO* OL maturation.**

(A, C) Coronal sections of P11 mouse cortex (CTX) and corpus callosum (CC). Hatched lines in panel C outlines CC boundaries. (B) Graphs quantifying the number of Olig2+ cells in CC and CTX. CC ns p = 0.0601, \*\*p = 0.0011, two-tailed unpaired t- test; CTX ns p = 0.1235, 1-way ANOVA Bonferroni's multiple comparison test, all 3 genotypes. n = 3 *WT;β-cat<sup>ex3</sup>*, 3 *Gde2KO;β-cat<sup>ex3</sup>*, 6 *Gde2KO;O-β-cat<sup>ex3</sup>*. (D) Graph quantifying the number of MBP+Olig2+ cells \*p = 0.0132, \*\*p = 0.0073, n = 3 *WT;β-cat<sup>ex3</sup>*, 3 *Gde2KO;β-cat<sup>ex3</sup>*, 6 *Gde2KO;O-β-cat<sup>ex3</sup>*. Two tailed unpaired Student's t-test. (E) Graphs quantifying number of CC1+ OLs. CC \*p = 0.0132, \*\*p = 0.0012; CTX \*p = 0.0242, \*\*\*p = 0.0008, n = 3 *WT;β-cat<sup>ex3</sup>*, 3 *Gde2KO;β-cat<sup>ex3</sup>*, 6 *Gde2KO;O-β-cat<sup>ex3</sup>*. Two tailed unpaired Student's t-test. All graphs: Mean  $\pm$  sem. Scale bars: 100  $\mu$ m.

**Figure S8**

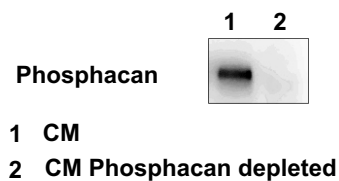
**A**

Protein name	Gene name	KO/WT ratio
Glycan-1;Secreted glycan-1	<i>Gpc1</i>	0.82
Glycan-2;Secreted glycan-2	<i>Gpc2</i>	0.91
Semaphorin-7A	<i>Sema7a</i>	0.94
Cadherin-13	<i>Cdh13</i>	0.95
Contactin-2 (a.k.a. TAG-1)	<i>Cntn2</i>	1.05
Neural cell adhesion molecule 1	<i>Ncam1</i>	1.11
RGM domain family member B	<i>Rgmb</i>	1.22
Lipoprotein lipase	<i>Lpl</i>	1.23
Repulsive guidance molecule A	<i>Rgma</i>	1.25
Contactin-1	<i>Cntn1</i>	1.25
Neural cell adhesion molecule 2	<i>Ncam2</i>	1.40

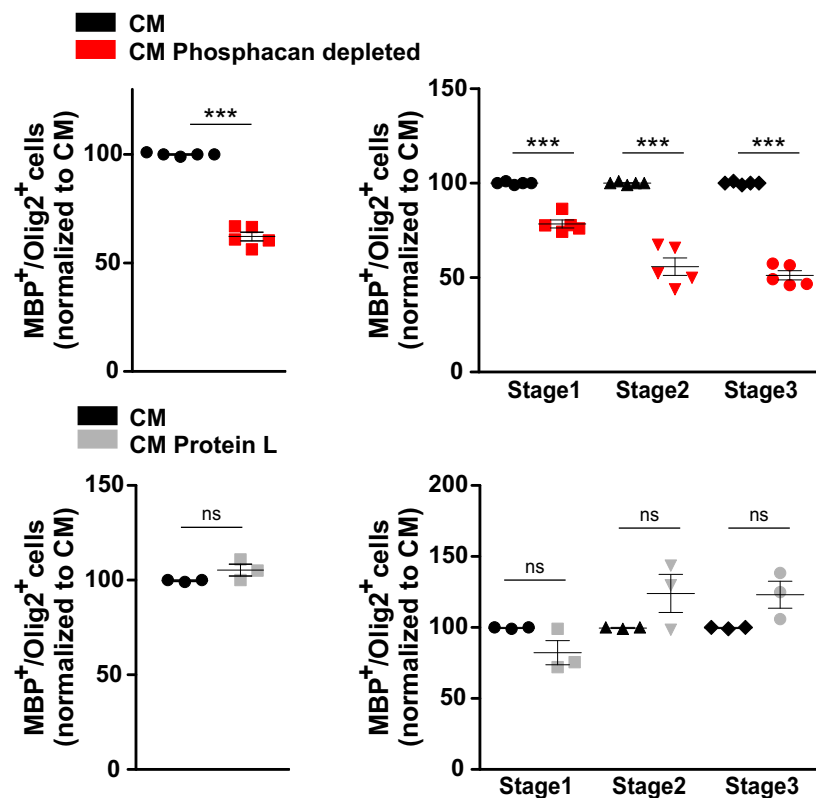
**B**

Protein name	Gene name	KO/WT ratio
Carboxypeptidase B2	<i>Cpb2</i>	0.33
Phosphatidylethanolamine-binding protein 1	<i>Pebp1</i>	0.43
Receptor-type tyrosine-protein phosphatase zeta	<i>Ptpz1</i>	0.44
Gamma-glutamyl hydrolase	<i>Ggh</i>	0.47
Follistatin-related protein 5	<i>Fstl5</i>	0.50
Glucose-6-phosphate isomerase	<i>Gpi</i>	0.51
ProSAsS	<i>Pcsk1n</i>	0.53
Noelin	<i>Olfm1</i>	0.53
Glia-derived nexin	<i>Serpine2</i>	0.54
Complement C5	<i>C5</i>	0.57
Collagen alpha-1(I) chain	<i>Col1a1</i>	3.98

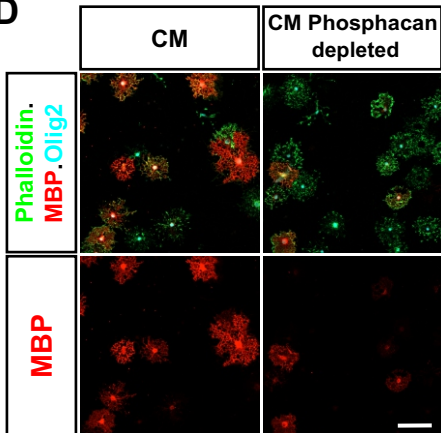
**C**



**E**



**D**



**F**

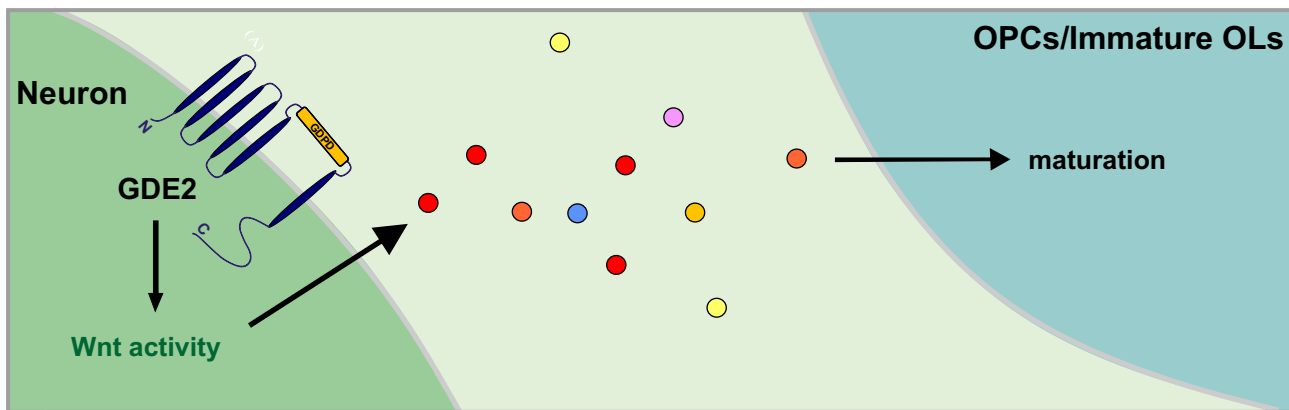


**Figure S8. Related to Figure 7. Candidate mechanisms for GDE2-dependent OL maturation.**

(A) List of GPI-anchored proteins identified in WT and *Gde2KO* CM by mass spectrometry. (B) List of secreted and extracellular matrix proteins identified in WT and *Gde2KO* CM by mass spectrometry. RPTPzeta (phosphacan) is highlighted in red. (C) Western blot of WT neuronal CM showing effective depletion of phosphacan using neuronal phosphacan antibodies conjugated to protein-L (D) Representative images of WT OPCs after culturing with WT neuronal CM and WT neuronal CM depleted for phosphacan. (E) Graphs quantifying the percentage of MBP+Olig2+ OLs (normalized to WT CM) in WT OPC cultures grown with WT neuronal CM or phosphacan depleted WT neuronal CM. Top panel \*\*\*p<0.0001, n = 5 WT CM, 5 Phosphacan depleted CM, two tailed unpaired t-test. All 3 stages of OL maturation are also affected (2-way ANOVA \*\*\*p < 0.0001; Bonferroni correction Stage 1 \*\*\*p <0.001; Stage 2 \*\*\*p <0.001; Stage 3 \*\*\*p <0.001; n = 5 WT CM, 5 Phosphacan depleted CM). No change in OPC maturation is observed between WT neuronal CM or WT neuronal CM preincubated with protein L alone. Bottom panel ns p = 0.1456, n = 3 WT CM, 3 Protein L incubated CM, two tailed unpaired t-test. Similarly, stages of OL maturation are unchanged (2-way ANOVA ns p = 0.1262; Bonferroni correction Stage 1 ns p >0.05; Stage 2 ns p >0.05; Stage 3 ns p >0.05; n = 5 WT CM, 5 Phosphacan depleted CM).(F) Model for GDE2 regulation of OL maturation. GDE2 stimulates canonical Wnt signaling in neurons. Wnt activation leads to release of neuronally-derived factors such as phosphacan, which act on neighboring OPCs or immature OLs to promote their maturation into myelinating oligodendrocytes.

**Table S1: Cell counts for in vitro cultures. Refers to Figure 4, Figure 7, and Figure S8.**

Fig 4	B/F	WT	<i>Gde2KO</i>	D/F			DIV3 CM	WT	<i>Gde2KO</i>
	DIV3+4 coculture			DIV3+4 CM	WT	<i>Gde2KO</i>			
Olig2+	2959		3030	Olig2+	1251	1126	Olig2+	730	907
MBP_stage 1	159		89	MBP_stage 1	251	194	MBP_stage 1	50	60
MBP_stage 2	116		43	MBP_stage 2	219	147	MBP_stage 2	71	51
MBP_Stage 3	53		18	MBP_Stage 3	62	30	MBP_Stage 3	48	27
total MBP+	328		152	total MBP+	532	371	total MBP+	169	138

Fig 7B

	<i>Gde2KO;β-Cat<sup>ex3</sup></i> CM	<i>Gde2KO;N-β-Cat<sup>ex3</sup></i> CM
Olig2+	936	894
MBP_stage 1	65	100
MBP_stage 2	26	43
MBP_Stage 3	17	28
total MBP+	108	171

Fig S8E

	CM	CM phsophacan depleted		CM	CM protein L
Olig2+	2189	2815	Olig2+	1007	869
MBP_stage 1	290	306	MBP_stage 1	132	97
MBP_stage 2	377	278	MBP_stage 2	132	140
MBP_Stage 3	189	138	MBP_Stage 3	61	67
total MBP+	856	722	total MBP+	325	304

**Table S3: Related to Supplemental Figure 8. List of proteins showing > 40% differential enrichment in Gde2KO CM.**

Number of altered protein expression: 149

Protein IDs	Protein names	Gene names	Sequence coverage KO [%]	Sequence coverage WT [%]	LFQ intensity KO	LFQ intensity WT	Ratio (KO/WT)
A8DUK4	beta-globin	Hbbt1	60.9	58.2	3.67E+06	3.93E+08	0.0093385
Q80ZV4	Cadherin-4	Cdh4	3.6	3.6	3.59E+05	6.73E+06	0.0533103
P35979	60S ribosomal protein L12	Olfm1	9.7	9.7	3.50E+05	3.35E+06	0.104707
Q3TLP8	Ras-related C3 botulinum toxin substrate 1	Rac1	9.45	12.3	1.22E+06	1.16E+07	0.1055619
P58283	E3 ubiquitin-protein ligase RNF216	Rnf216	0.8	0.8	7.20E+05	5.81E+06	0.1241085
Q6ZWQ9	Myosin regulatory light chain 12B	Myl12a	17.4	9.3	2.92E+06	2.11E+07	0.1384735
P48678	Prelamin-A/C	Lmna	1.8	0.75	7.71E+04	3.94E+05	0.1955637
F6VYE2	Zinc finger MYM-type protein 4	Zmym4	0.7	0.7	3.81E+07	1.28E+08	0.2985482
G5E866	Splicing factor 3B subunit 1	Sf3b1	0.35	1.1	6.29E+05	2.08E+06	0.3018324
Q99J16	Ras-related protein Rap-1b	Rap1b	11.15	11.15	2.20E+06	7.24E+06	0.304105
P62897	Cytochrome c, somatic	Cycs	17.15	17.15	1.47E+06	4.78E+06	0.3074461
P32233	Developmentally-regulated GTP-binding protein 1	Drg1	4.4	4.4	4.55E+05	1.37E+06	0.3315903
Q2KIG3	Carboxypeptidase B2	Cpb2	2.6	2.15	2.81E+05	8.34E+05	0.3367496
P19253	60S ribosomal protein L13a	Rpl13a	8.1	8.1	1.20E+06	3.52E+06	0.3409558
P97350	Plakophilin-1	Pkp1	2.25	2.25	2.43E+06	6.66E+06	0.3647232
P62242	40S ribosomal protein S8	Rps8	8.9	7.2	7.11E+05	1.75E+06	0.4058655
Q3UHN9	Bifunctional heparan sulfate N-deacetylase	Ndst1	0.8	1.6	9.53E+05	2.35E+06	0.4063519
A0A087WPL5	ATP-dependent RNA helicase A	Dhx9	0.6	0.85	4.55E+05	1.11E+06	0.4094201
Q8QZY9	Splicing factor 3B subunit 4	Sf3b4	1.65	3.3	2.16E+06	5.03E+06	0.4288
P70296	Phosphatidylethanolamine-binding protein 1	Pebp1	32.6	29.15	4.56E+07	1.05E+08	0.4363098
Q62189	U1 small nuclear ribonucleoprotein A	Snrp1a	9.55	9.55	7.22E+06	1.64E+07	0.4395122
B9EKR1	Receptor-type tyrosine-protein phosphatase zeta	Ptpz1	7.05	6.8	1.08E+08	2.43E+08	0.445375
Q9DBG3	AP-2 complex subunit beta;AP complex subunit beta	Ap2b1	2	1.3	2.06E+06	4.55E+06	0.4524362
Q60648	Ganglioside GM2 activator	Gm2a	8.8	4.4	1.39E+06	2.98E+06	0.4666868
Q9CXV9	DCN1-like protein 5	Dcn1d5	6.3	6.3	3.76E+07	8.06E+07	0.466781
Q9Z0L8	Gamma-glutamyl hydrolase	Ggh	12.9	12.9	6.49E+06	1.37E+07	0.4751144
P80317	T-complex protein 1 subunit zeta	Cct6a	4.35	2.85	1.13E+06	2.35E+06	0.4792104
B1AX58	Plastin-3	Pls3	0.7	1.4	8.46E+05	1.76E+06	0.4811927
Q9R1P3	Proteasome subunit beta type-2	Psmb2	6.2	9.95	8.15E+06	1.65E+07	0.4936686
Q8R093	Uridine phosphorylase	Upp2	4.2	2.1	5.18E+07	1.03E+08	0.5007006
Q8BFR2	Follistatin-related protein 5	Fstl5	8	9.8	1.04E+07	2.08E+07	0.5017444
Q9EST1	Gasdermin-A	Gsdma	1	2.6	1.80E+06	3.50E+06	0.5148759
Q91V64	Isochorismatase domain-containing protein 1	Isoc1	5.2	10.4	1.33E+06	2.58E+06	0.5164249
P06745	Glucose-6-phosphate isomerase	Gpi	5.2	5.2	9.57E+05	1.84E+06	0.5188111
Q9CQU0	Thioredoxin domain-containing protein 12	Txndc12	6.45	4.4	1.93E+06	3.68E+06	0.5235417
Q08331	Calretinin	Calb2	11.8	11.8	3.97E+06	7.51E+06	0.5290136
Q9QXV0	ProSAAS	Pcsk1n	12.2	10.5	9.84E+06	1.85E+07	0.53233
A3KGE4	Noelin	Olfm1	4.3	4.3	7.73E+05	1.44E+06	0.5356937
Q3TKX1	V-type proton ATPase subunit S1	Atp6ap1	14.2	14.2	1.28E+07	2.37E+07	0.5403885
Q9DAY9	Nucleophosmin	Npm1	4.1	14	1.17E+07	2.15E+07	0.5426547
Q07235	Glia-derived nexin	Serpine2	13.35	13.35	5.49E+06	1.00E+07	0.5480371
Q9JJU8	SH3 domain-binding glutamic acid-rich-like protein	Sh3bgrl	25	18	7.48E+06	1.36E+07	0.548844
P61164	Alpha-centrin	Actr1a	12.95	7.85	1.46E+06	2.65E+06	0.550069
P61358	60S ribosomal protein L27	Rpl27	7.35	10.65	2.31E+06	4.20E+06	0.5504141
O09061	Proteasome subunit beta type-1	Psmb1	14.15	18.3	1.62E+07	2.92E+07	0.5534894
Q5RKN9	F-actin-capping protein subunit alpha-1	Capza1	13.6	13.6	4.36E+06	7.85E+06	0.5548677
E9PYH2	Cytosolic acyl coenzyme A thioester hydrolase	Acot7	8.3	6.75	6.44E+06	1.15E+07	0.559416
P24369	Peptidyl-prolyl cis-trans isomerase B	Ppib	18.05	16	2.04E+07	3.62E+07	0.5644408
Q9D1C8	Vacuolar protein sorting-associated protein 28 homolog	Vps28	2.75	5.5	7.42E+05	1.31E+06	0.5652669
Q3TX55	Actin-related protein 2/3 complex subunit 4	Arpc4	20.25	17.9	1.39E+07	2.44E+07	0.569117
P62702	40S ribosomal protein S4	Gm15013	5.1	8.1	7.23E+06	1.27E+07	0.569801
S4R1N6	40S ribosomal protein S18	Rps18	22.9	18.7	1.08E+07	1.88E+07	0.5729743
P06684	Complement C5	C5	1.05	1.05	2.07E+06	3.60E+06	0.5752787
D3Z6E4	Enolase/Gamma-enolase	Eno2	6.35	7.9	4.46E+05	7.64E+05	0.5833966
P50247	Adenosylhomocysteinase	Ahcy	9	9	5.44E+06	9.19E+06	0.5925307
P20029	78 kDa glucose-regulated protein	Hspa5	7.25	9.4	2.20E+06	3.68E+06	0.5991105
P55821	Stathmin-2	Stmn2	14.5	14.5	2.67E+07	1.91E+07	1.4007286
O35136	Neural cell adhesion molecule 2	Ncam2	3.5	3.5	2.09E+06	1.49E+06	1.4047028
Q60994	Adiponectin	Adipoq	10.75	10.75	7.19E+07	5.10E+07	1.4090303
Q60864	Stress-induced-phosphoprotein 1	Stip1	2.9	2.9	5.38E+06	3.81E+06	1.4108147
D3YYE1	Acidic leucine-rich nuclear phosphoprotein 32 family member A	Anp32a	13.9	17.2	1.19E+07	8.38E+06	1.4150217
Q8BGQ7	Alanine-tRNA ligase, cytoplasmic	Aars	0.9	0.9	1.01E+06	7.09E+05	1.4222222
Q93092	Transaldolase	Taldo1	14	11.5	1.43E+08	9.97E+07	1.4302839
Q99J36	THUMP domain-containing protein 1	Thumpd1	8.45	7.3	2.46E+06	1.72E+06	1.434379
Q99PT1	Rho GDP-dissociation inhibitor 1	Arhgdia	29.9	30.15	8.03E+07	5.58E+07	1.4393366
Q61598	Rab GDP dissociation inhibitor beta	Gdi2	17.75	16.95	5.91E+07	4.07E+07	1.4504449
A2A418	Amine oxidase	Aoc3	1.9	1.9	1.04E+08	7.17E+07	1.45059
P08030	Adenine phosphoribosyltransferase	Aprt	10	7.2	4.33E+06	2.98E+06	1.4560516
P21460	Cystatin-C	Cst3	27.5	27.5	5.77E+08	3.93E+08	1.4677356
P35441	Thrombospondin-1	Thbs1	4.8	5	6.15E+06	4.14E+06	1.4860469
P04444	Hemoglobin subunit beta-H1	Hbb-bh1	21.1	21.1	7.56E+06	5.08E+06	1.4896048
P02104	Hemoglobin subunit epsilon-Y2	Hbb-y	40.15	39.15	2.39E+08	1.60E+08	1.4902499
Q8CBG6	6-phosphogluconactonase	Pgls	7.2	10.9	4.86E+06	3.26E+06	1.4918735
P63158	High mobility group protein B1	Hmgb1	24.3	24	5.03E+07	3.37E+07	1.4921339
Q564E2	L-lactate dehydrogenase	Ldha	32.5	32.5	1.43E+08	9.51E+07	1.5027012
P34022	Ran-specific GTPase-activating protein	Ranbp1	8.1	10.8	5.39E+06	3.58E+06	1.5047218
P62869	Transcription elongation factor B polypeptide 2	Tceb2	26.25	22	7.90E+06	5.24E+06	1.5070908
O70251	Elongation factor 1-beta	Eef1b2	11.7	15.2	6.12E+06	4.03E+06	1.5189003
Q9WU60	Attractin	Atn	0.55	0.55	2.72E+06	1.78E+06	1.5249867

A2AI62	Hephaestin	<i>Heph</i>	0.9	0.9	6.04E+07	3.94E+07	1.5319845
Q5XJF6	Ribosomal protein	<i>Rpl10a</i>	12.4	12.4	1.26E+07	8.16E+06	1.5469304
Q9WTP6	Adenylate kinase 2	<i>Ak2</i>	6.9	4.2	6.54E+05	4.19E+05	1.560639
P21619	Lamin-B2	<i>Lmnb2</i>	2.3	1.15	8.17E+05	5.23E+05	1.5621844
P10126	Elongation factor 1-alpha 1	<i>Eef1a1</i>	15.35	12.75	2.10E+09	1.33E+09	1.5713376
Q5SXR6	Clathrin heavy chain;Clathrin heavy chain 1	<i>Cltc</i>	10.55	10.15	6.69E+07	4.26E+07	1.5719838
Q9CQI6	Coactosin-like protein	<i>Cotl1</i>	14.45	16.55	1.03E+08	6.50E+07	1.5812476
Q6P1J1	Dihydropyrimidinase-related protein 1	<i>Crmp1</i>	6.15	6.15	5.37E+06	3.38E+06	1.5860785
B2M1R7	Poly(rC)-binding protein 2	<i>Pcbp2</i>	14.25	13.85	1.76E+07	1.11E+07	1.5870965
Q9DCD0	6-phosphogluconate dehydrogenase, decarboxylating	<i>Pgd</i>	5.8	5.8	1.23E+07	7.69E+06	1.6018917
Q8BHZ0	Protein FAM49A	<i>Fam49a</i>	8.5	6.5	7.84E+05	4.87E+05	1.6099238
P35585	AP-1 complex subunit mu-1	<i>Ap1m1</i>	5.8	4.05	1.90E+06	1.17E+06	1.627294
Q61171	Peroxiredoxin-2	<i>Prdx2</i>	25	25	5.06E+08	3.10E+08	1.6326191
F6ZBL2	E3 ubiquitin-protein ligase MIB1	<i>Mib1</i>	2.5	2.5	1.95E+09	1.18E+09	1.6437232
Q3U3V1	Coagulation factor X	<i>F10</i>	1.8	1.8	3.78E+06	2.28E+06	1.6583261
Q8BTU6	Eukaryotic initiation factor 4A-II	<i>Eif4a2</i>	24.2	21.65	9.47E+06	5.57E+06	1.6980858
P43277	Histone H1.3	<i>Hist1h1d</i>	18.55	18.55	2.84E+08	1.67E+08	1.6982031
Q91WU0	Carboxylic ester hydrolase	<i>Cesf1</i>	2.1	2.1	6.60E+07	3.84E+07	1.7195086
E0CZ27	Histone H3	<i>H3f3a</i>	15.55	19.3	5.70E+08	3.30E+08	1.7248706
E9Q6B6	C-Jun-amino-terminal kinase-interacting protein 3	<i>Mapk8ip3</i>	1.4	1.4	3.23E+07	1.86E+07	1.7333405
Q8BIZ0	Protocadherin-20	<i>Pcdh20</i>	0.7	0.7	6.59E+05	3.79E+05	1.7368837
P29788	Vitronectin	<i>Vtn</i>	3.8	3.8	2.38E+06	1.35E+06	1.7573225
Q9CQV8	14-3-3 protein beta/alpha	<i>Ywhab</i>	20.9	23.15	4.20E+07	2.38E+07	1.7635641
P17897	Lysozyme C-1	<i>Lyz1</i>	8.1	8.1	3.90E+06	2.19E+06	1.7755069
P97333	Neuropilin-1	<i>Nrp1</i>	2.3	3.1	3.55E+06	1.99E+06	1.7817533
G3X914	Aly/REF export factor 2	<i>Alyref2</i>	5	5	1.75E+07	9.73E+06	1.8022802
P63260	Actin	<i>Actg1</i>	47.6	44.65	3.53E+06	1.94E+06	1.8262027
P62082	40S ribosomal protein S7	<i>Rps7</i>	2.1	2.1	7.19E+06	3.94E+06	1.8266545
H7BX52	Cullin-2	<i>Cul2</i>	17.8	17.8	5.21E+06	2.85E+06	1.8277042
Q9R1P1	Proteasome subunit beta type-3	<i>Psmb3</i>	6.8	3.4	6.64E+06	3.63E+06	1.8284916
F6W8R9	Nesprin-2	<i>Syne2</i>	1.1	0.55	7.38E+06	4.00E+06	1.843401
Q8VEK3	Heterogeneous nuclear ribonucleoprotein U	<i>Hnrnpu</i>	4.65	4.65	5.36E+06	2.89E+06	1.8557495
A2A813	Protein deglycase DJ-1	<i>Park7</i>	9.1	7.7	7.71E+06	4.15E+06	1.8572581
G3UZR0	N(G),N(G)-dimethylarginine dimethylaminohydrolase 2	<i>Ddah2</i>	16.55	19.7	3.48E+06	1.87E+06	1.8595037
P2604	Moesin	<i>Msn</i>	4.75	4.75	3.57E+06	1.91E+06	1.8641588
Q9JMG7	Hepatoma-derived growth factor-related protein 3	<i>Hdgfrp3</i>	8.2	8.2	2.53E+06	1.34E+06	1.8807877
D3Z7E6	Platelet-activating factor acetylhydrolase IB subunit gamma	<i>Pafah1b3</i>	13.9	16.4	8.71E+06	4.61E+06	1.8873094
Q5SW88	Ras-related protein Rab-1A	<i>Rab1</i>	8.9	12.4	1.80E+07	9.38E+06	1.9214568
Q61233	Plastin-2	<i>Lcp1</i>	9	6.45	1.52E+07	7.75E+06	1.9644182
D3Z315	Coatomer subunit epsilon	<i>Cope</i>	7.3	9.9	1.54E+06	7.76E+05	1.9872323
P26645	Myristoylated alanine-rich C-kinase substrate	<i>Marcks</i>	16.2	8.1	5.31E+06	2.52E+06	2.1103271
Q62084	Protein phosphatase 1 regulatory subunit 14B	<i>Ppp1r14b</i>	17	17.35	8.34E+06	3.89E+06	2.1448012
G3UY42	Polyadenylate-binding protein 2	<i>Pabpn1</i>	8.5	8.5	2.45E+06	1.12E+06	2.1813408
B7FAV1	Filamin-A	<i>Flna</i>	1	0.3	2.64E+06	1.19E+06	2.217373
Q9CQI3	Glia maturation factor beta	<i>Gmfb</i>	14.6	14.6	1.14E+07	5.01E+06	2.267461
H7BXC3	Triosephosphate isomerase	<i>Tpi1</i>	12.9	12.6	4.71E+06	2.07E+06	2.2687512
Q60865	Caprin-1	<i>Caprin1</i>	3.3	3.3	2.74E+07	1.20E+07	2.2891093
F6Q2E3	26S protease regulatory subunit 6A	<i>Psmc3</i>	7.9	3.95	6.35E+05	2.72E+05	2.3318521
F6VR16	Ubiquitin-like modifier-activating enzyme 5	<i>Uba5</i>	16.2	8.1	5.56E+05	2.33E+05	2.383202
P60867	40S ribosomal protein S20	<i>Rps20</i>	14.25	9.65	1.46E+07	6.10E+06	2.3875143
Q14AA6	GTP-binding nuclear protein Ran	<i>Ran</i>	9.7	14.8	5.11E+07	2.13E+07	2.3989767
P68134	Actin, alpha skeletal muscle	<i>Acta1</i>	26.4	23.45	8.55E+07	3.55E+07	2.4108667
P35700	Peroxiredoxin-1	<i>Prdx1</i>	17.75	20.15	6.77E+07	2.75E+07	2.4657958
P02089	Hemoglobin subunit beta-2	<i>Hbb-b2</i>	46.9	46.6	1.84E+08	7.40E+07	2.4912119
Q04750	DNA topoisomerase 1	<i>Top1</i>	2.1	2.1	1.98E+06	7.37E+05	2.6873618
Q543K9	Purine nucleoside phosphorylase	<i>Pnp;Pnp2</i>	6.6	3.3	7.72E+05	2.84E+05	2.7204358
Q8CGP4	Histone H2A	<i>Hist1h2aa</i>	21.4	21.4	4.88E+08	1.74E+08	2.8048444
P83917	Chromobox protein homolog 1	<i>Cbx1</i>	9.2	7.55	1.22E+06	4.26E+05	2.8537753
O35864	COP9 signalosome complex subunit 5	<i>Cops5</i>	14.3	14.3	4.69E+06	1.63E+06	2.8804678
Q9CR00	26S proteasome non-ATPase regulatory subunit 9	<i>Psmrd9</i>	5.1	2.55	4.20E+06	1.36E+06	3.0804593
P00015	Cytochrome c, testis-specific	<i>Cytc</i>	24.3	17.65	1.89E+07	5.88E+06	3.2051827
P28658	Ataxin-10	<i>Atxn10</i>	1.45	1.45	8.12E+05	2.29E+05	3.5437179
P20357	Microtubule-associated protein 2	<i>Map2</i>	1.75	1.4	4.00E+06	1.13E+06	3.5489953
P61750	ADP-ribosylation factor 4	<i>Arf4</i>	11.7	11.7	9.87E+06	2.49E+06	3.955426
P11087	Collagen alpha-1(I) chain	<i>Col1a1</i>	6.15	3.95	1.68E+07	4.21E+06	3.9850303
P97379	Ras GTPase-activating protein-binding protein 2	<i>G3bp2</i>	12	12	3.87E+06	9.04E+05	4.278474
D3Z7K0	Ubiquitin thioesterase OTUB1	<i>Otub1</i>	18.65	14.9	2.72E+07	5.13E+06	5.3105051
P27048	Small nuclear ribonucleoprotein-associated protein B	<i>Snrpb</i>	8.25	3.25	1.68E+06	2.01E+05	8.3721104
P35396	Peroxisome proliferator-activated receptor delta	<i>Ppard</i>	1.6	1.6	1.39E+08	1.00E+07	13.877689
P07309	Transthyretin	<i>Ttr</i>	11.9	5.1	7.35E+07	1.55E+06	47.408315